Available online at www.sciencedirect.com
ScienceDirect
Optics Communications 269 (2007) 362–369
OPTICS COMMUNICATIONS
www.elsevier.com/locate/optcom

Sub-Doppler spectral resolution in a resonantly driven four-level coherent medium

L.B. Kong [a,b,c,*], X.H. Tu [a,b], J. Wang [a,b], Yifu Zhu [d], M.S. Zhan [a,b]

[a] State Key Laboratory of Magnetic Resonance and Atomic and Molecular Physics, Wuhan Institute of Physics and Mathematics, Chinese Academy of Sciences, Wuhan 430071, People's Republic of China
[b] Center for Cold Atom Physics, Chinese Academy of Sciences, Wuhan 430071, People's Republic of China
[c] Graduate School, Chinese Academy of Sciences, Beijing 100080, People's Republic of China
[d] Department of Physics, Florida International University, Miami, FL 33199, USA

Received 7 March 2006; received in revised form 16 July 2006; accepted 17 August 2006

Abstract

Sub-Doppler spectral resolution has been studied in Doppler-broadened multi-level ^{87}Rb atoms coherently coupled by two strong laser fields. Narrow spectral features of absorption or gain are observed in the center or sides of the Doppler-broadened absorption profile. Analytical and numerical calculations based on a four-level N type model are presented to explain the experimental results.

PACS: 42.50.Gy; 42.50.Fx; 42.62.Fi

1. Introduction

When a multi-level atomic medium is driven by laser fields, the induced atomic coherence and interference may modify the dispersive and absorptive properties of the atomic medium and leads to a variety of interesting phenomena for fundamental studies and practical applications, such as electromagnetically induced transparency (EIT) [1,2], coherent population trapping (CPT) [3], lasing without population inversion (LWI) [4], subluminal [5] or superluminal light [6] propagation, light storage [7], and coherent nonlinear optics at low light levels [8,10].

Atomic vapors are often used to study the atomic coherence and interference. At room temperatures, the Doppler broadening dominates the linewidth of the atomic transitions and generally reduces the coherent effects. A direct way to overcome the Doppler broadening is to use cold atoms. For hot atoms, it is well known that Doppler-free configurations can be realized for certain laser–atom coupling schemes by arranging the propagation directions of laser beams. It has been shown that sub-Doppler and even sub-natural linewidths can be observed in Doppler-broadened, coherently driven atomic systems [11–22], which may lead to useful applications in laser frequency stabilization, gas-cell atomic frequency standards, narrow-band optical sources, and so on.

In this paper, we report an experimental study of the sub-Doppler spectral resolution in a Doppler-broadened four-level atomic medium interacting with three lasers. The generic four-level atomic system is shown schematically in Fig. 1a, in which a weak laser field E_p drives the $|1\rangle \rightarrow |3\rangle$ transition and two intense laser fields E_c and E_b couple the transitions $|2\rangle \rightarrow |3\rangle$ and $|1\rangle \rightarrow |4\rangle$, respectively. The four-level atomic system is approximately realized with a multi-level ^{87}Rb system shown in Fig. 1b. We note that similar four-level N systems have been theoretically studied in Na_2 molecules [15] and also used as a simplified model to explain the electromagnetically induced absorption (EIA)

* Corresponding author. Address: Wuhan Institute of Physics and Mathematics, Chinese Academy of Sciences, Wuhan 430071, People's Republic of China. Tel.: +86 2787199615; fax: +86 2787199291.
E-mail addresses: konglingbo@wipm.ac.cn (L.B. Kong), mszhan@wipm.ac.cn (M.S. Zhan).

0030-4018/$ - see front matter © 2006 Elsevier B.V. All rights reserved.
doi:10.1016/j.optcom.2006.08.017

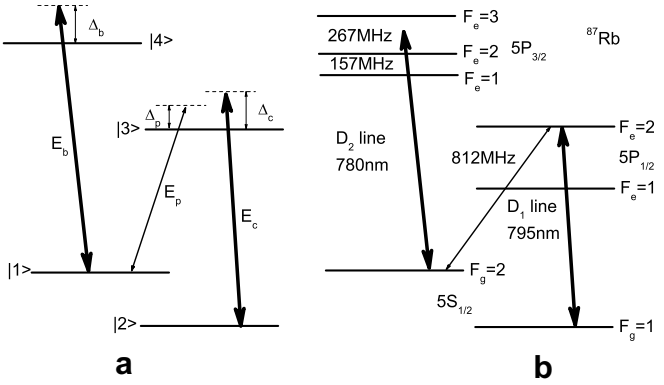

Fig. 1. (a) Four-level N-type scheme. (b) Energy-level diagram of ^{87}Rb atoms.

in degenerate two-level atomic systems [21,22]. The experimental work have been also performed in solid [24] and in cold atoms [25].

Here we present an experimental study of the four-level N system in Doppler-broadened ^{87}Rb atomic vapors. In a co-propagating geometry of the three lasers, we measure the probe absorption spectra in this system. When the $|4\rangle \rightarrow |2\rangle$ transition is dipole forbidden (no spontaneous decay from $|4\rangle$ to $|2\rangle$), we observe the sub-Doppler absorption peaks and dips near the center of Doppler-broadened absorption profile of the $|1\rangle \rightarrow |3\rangle$ probe transition; if the $|4\rangle \rightarrow |2\rangle$ transition is dipole allowed (with a spontaneous decay rate γ_{42} from $|4\rangle$ to $|2\rangle$), we observe the sub-Doppler amplification of the probe laser in the center of the $|1\rangle \rightarrow |3\rangle$ transition. The narrow spectral features of the observed absorption and gain approach the natural linewidth. Similar sub-Doppler spectral peaks and dips are also observed when the two intense coupling lasers are detuned from the respective resonances. In order to understand the underlying physical mechanism of the observed sub-Doppler spectral measurements, we perform analytical and numerical calculations based on the four-level atomic system of Fig. 1a, which agree well with the experimental results.

2. Experimental results and theoretical analysis

We perform the experiment with ^{87}Rb atoms in a vapor cell at room temperatures. The ^{87}Rb energy-level structure and the laser coupling scheme are shown in Fig. 1b. An extended-cavity diode laser tuned to the D1 $5S_{1/2}$, $F_g = 1 \rightarrow 5P_{1/2}$, $F_e = 2$ transition at 795 nm serves as the coupling field E_c. Another extended-cavity diode laser at 795 nm is used as the weak probe field E_p and is scanned across the D1 $5S_{1/2}$, $F_g = 2 \rightarrow 5P_{1/2}$, $F_e = 2$ transition. The hyperfine splitting between the excited level $5P_{1/2}$, $F_e = 2$ and $F_e = 1$ is 812 MHz, which is greater than the Doppler width (~540 MHz) of the rubidium vapor at room temperatures. Therefore, the Doppler-broadened absorption lines for the two transitions ($5S_{1/2}$, $F_g = 2 \rightarrow 5P_{1/2}$, $F_e = 2$ and $F_e = 1$) are well resolved. A third extended-cavity diode laser at 780 nm is used as the second coupling field E_b and is tuned to the D2 $5S_{1/2}$, $F_g = 2 \rightarrow 5P_{3/2}$, $F_e = 1, 2, 3$ transitions. The three hyperfine levels of the excited states $5P_{3/2}$, $F_e = 1, 2, 3$ are separated by 157 and 267 MHz, respectively (Fig. 1b).

The experimental arrangement is shown schematically in Fig. 2. Natural mixture of ^{87}Rb and ^{85}Rb isotopes is contained in a 10-cm long cylindrical quartz cell without buffer gas. The estimated rubidium atomic density is on the order of 10^{10} atoms/cm^3. Three lasers co-propagate through the vapor cell. The two coupling lasers have the same linear polarization and are overlapped by a beam splitter. The probe laser is polarized perpendicular to that of the two coupling lasers. The probe laser and two coupling lasers are overlapped in a PBS and pass through the vapor cell. The probe laser beam is separated from the two coupling laser beams outside the cell by another PBS and is detected by a photodiode. The powers of the lasers are controlled by neutral density filters. During the experiment, the power of the probe laser is kept below 5 μW.

Fig. 3 shows the measured absorption spectra of the probe laser versus the probe frequency detuning Δ_p. When the coupling field E_c is on resonance ($\Delta_c = 0$) and the second coupling field E_b is turned off, the coupled ^{87}Rb system forms a standard three-level Λ type configuration and we observe the EIT spectrum with a narrow dip in the center of the Doppler absorption profile of the $5S_{1/2}$, $F_g = 2 \rightarrow 5P_{1/2}$, $F_e = 2$ transition as shown in Fig. 3a. When the second coupling field E_b with the same intensity as that of the first coupling field E_c is turned on and tuned on resonance with the $5S_{1/2}$, $F_g = 2 \rightarrow 5P_{3/2}$, $F_e = 3$ transition, a narrow absorption peak in the line center of Doppler-broadened EIT profile is observed as shown in Fig. 3b. Since the $5S_{1/2}$, $F_g = 1 \rightarrow 5P_{3/2}$, $F_e = 3$ transition is a dipole forbidden transition (with the selection rules $\Delta F = 0, \pm 1$), there is no spontaneous decay from the excited state $|4\rangle$ ($5P_{3/2}$, $F_e = 3$) to the ground state $|2\rangle$ ($5S_{1/2}$, $F_g = 1$). On the other hand, when the coupling field E_b is tuned on resonance with the $5S_{1/2}$, $F_g = 2 \rightarrow 5P_{3/2}$, $F_e = 2$ (or 1) transition, it opens the spontaneous decay channel $|4\rangle$ ($5P_{3/2}$, $F_e = 2$ or 1) to $|2\rangle$ ($5S_{1/2}$, $F_g = 2$). We then find that as the intensity of the coupling

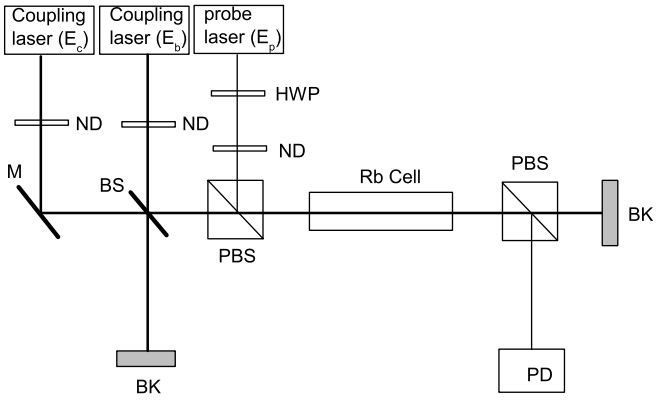

Fig. 2. Experimental setup: ND, natural density filter; M, mirror; BS, beam splitter; BK, beam blocker; HWP, half-wave plate; PBS, polarization beam spilitter; and PD, photo detector.

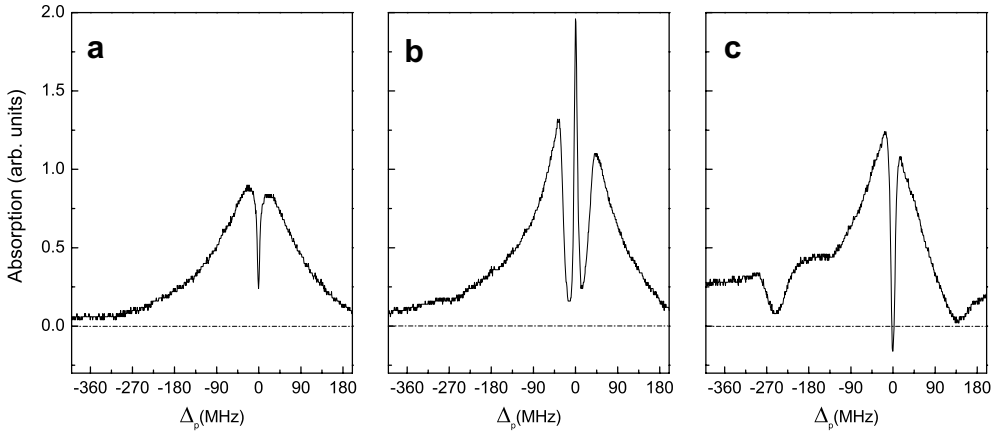

Fig. 3. Measured probe absorption spectra versus the probe frequency detuning Δ_p. The coupling laser E_c is always tuned on resonance with $5S_{1/2}$, $F_g = 1 \rightarrow 5P_{1/2}$, $F_e = 2$ transition and has an intensity of 18 mW/cm^2: (a) Three-level Λ type EIT spectrum (the coupling laser E_b is turned off). (b) The coupling laser E_b (with the same intensity as that of the coupling laser E_c) is on and tuned to the resonance of the $5S_{1/2}$, $F_g = 2 \rightarrow 5P_{3/2}$, $F_e = 3$ transition. (c) The coupling laser E_b is tuned to the resonance of the $5S_{1/2}$, $F_g = 2 \rightarrow 5P_{3/2}$, $F_e = 2$ transition and with an intensity $\sim$32 mW/cm^2.

laser field E_b increases, the observed narrow EIT dip in the line center of Doppler-broadened absorption profile in Fig. 3a becomes deeper and evolves from absorption into amplification as shown in Fig. 3c.

We note that the narrow absorption peak in the center of the Doppler absorption profile of Fig. 3b (without spontaneous decay γ_{42}) resembles electromagnetically induced absorption (EIA) [18–22], but its physical origin is different from EIA. The basic EIA model is based on an open four-level configuration within a degenerate two-state system, in which transfer of coherence (TOC) [19–21] or transfer of population (TOP) [19,22] is essential. The four-level N type system studied here is non-degenerate and is closed, and is similar to the N type system analyzed in Ref. [21] without TOC. In our experiment, the co-propagating geometry of three laser beams results in the sub-Doppler spectral resolution. In addition to the spectrum of a single narrow absorption peak or dip, we also observe the multiple narrow absorption peaks and dips by varying the relative intensity of the two coupling lasers. These spectra will be discussed along with the theoretical analysis presented below.

The density matrix equations for the four-level system (Fig. 1a) under the dipole and rotating-wave approximation are written as

$$\dot{\rho}_{11} = \gamma_{31}\rho_{33} + \gamma_{41}\rho_{44} - \frac{i}{2}\Omega_p\rho_{13} + \frac{i}{2}\Omega_p^*\rho_{31} - \frac{i}{2}\Omega_b\rho_{14} + \frac{i}{2}\Omega_b^*\rho_{41}, \tag{1a}$$

$$\dot{\rho}_{22} = \gamma_{32}\rho_{33} + \gamma_{42}\rho_{44} - \frac{i}{2}\Omega_c\rho_{23} + \frac{i}{2}\Omega_c^*\rho_{32}, \tag{1b}$$

$$\dot{\rho}_{33} = -\gamma_3\rho_{33} + \frac{i}{2}\Omega_p\rho_{13} - \frac{i}{2}\Omega_p^*\rho_{31} + \frac{i}{2}\Omega_c\rho_{23} - \frac{i}{2}\Omega_c^*\rho_{32}, \tag{1c}$$

$$\dot{\rho}_{44} = -\gamma_4\rho_{44} + \frac{i}{2}\Omega_b\rho_{14} - \frac{i}{2}\Omega_b^*\rho_{41}, \tag{1d}$$

$$\dot{\rho}_{14} = -\Gamma_{14}\rho_{14} + \frac{i}{2}\Omega_p^*\rho_{34} + \frac{i}{2}\Omega_b^*(\rho_{44} - \rho_{11}), \tag{1e}$$

$$\dot{\rho}_{21} = -\Gamma_{21}\rho_{21} - \frac{i}{2}\Omega_p\rho_{23} - \frac{i}{2}\Omega_b\rho_{24} + \frac{i}{2}\Omega_c^*\rho_{31}, \tag{1f}$$

$$\dot{\rho}_{23} = -\Gamma_{23}\rho_{23} + \frac{i}{2}\Omega_c^*(\rho_{33} - \rho_{22}) - \frac{i}{2}\Omega_p^*\rho_{21}, \tag{1g}$$

$$\dot{\rho}_{24} = -\Gamma_{24}\rho_{24} + \frac{i}{2}\Omega_c^*\rho_{34} - \frac{i}{2}\Omega_b^*\rho_{21} \tag{1h}$$

$$\dot{\rho}_{31} = -\Gamma_{31}\rho_{31} - \frac{i}{2}\Omega_p(\rho_{33} - \rho_{11}) - \frac{i}{2}\Omega_b\rho_{34} + \frac{i}{2}\Omega_c\rho_{21}, \tag{1i}$$

$$\dot{\rho}_{34} = -\Gamma_{34}\rho_{34} + \frac{i}{2}\Omega_p\rho_{14} + \frac{i}{2}\Omega_c\rho_{24} - \frac{i}{2}\Omega_b^*\rho_{31}, \tag{1j}$$

where

$$\Gamma_{14} = (\gamma_4 + \gamma_{21})/2 + i\Delta_b, \quad \Gamma_{21} = \gamma_{21} - i(\Delta_p - \Delta_c),$$
$$\Gamma_{23} = (\gamma_3 + \gamma_{21})/2 + i\Delta_c, \quad \Gamma_{24} = (\gamma_4 + \gamma_{21})/2 + i(\Delta_b - \Delta_p + \Delta_c),$$
$$\Gamma_{31} = (\gamma_3 + \gamma_{21})/2 - i\Delta_p, \quad \Gamma_{34} = (\gamma_3 + \gamma_4)/2 + i(\Delta_b - \Delta_p).$$

$\Delta_p = \omega_p - \omega_{31}$, $\Delta_c = \omega_c - \omega_{32}$, and $\Delta_b = \omega_b - \omega_{41}$ are single-photon detunings of the probe laser E_p, the first coupling laser E_c and the second coupling laser E_b with the transitions $|1\rangle \rightarrow |3\rangle$, $|3\rangle \rightarrow |2\rangle$ and $|4\rangle \rightarrow |1\rangle$, respectively. $\Omega_p = \mu_{31}E_p/\hbar$, $\Omega_c = \mu_{32}E_c/\hbar$ and $\Omega_b = \mu_{41}E_b/\hbar$ are Rabi frequencies, with μ_{mn} (m, $n = 1,2,3,4$) denoting the dipole moment for the corresponding transition $|m\rangle \rightarrow |n\rangle$, respectively. γ_{31} (γ_{32}) and γ_{41} (γ_{42}) are spontaneous decay rates from the excited states $|4\rangle$ and $|3\rangle$ to the ground state $|1\rangle$ ($|2\rangle$), respectively. The natural linewidths of the excited $|3\rangle$ and $|4\rangle$ states for ^{87}Rb atoms are $\gamma_3 = 2\pi \times 5.3$ MHz ($\gamma_3 = \gamma_{31} + \gamma_{32}$) and $\gamma_4 = 2\pi \times 5.9$ MHz ($\gamma_4 = \gamma_{41} + \gamma_{42}$), respectively. γ_{21} is the dephasing rate between the ground states $|1\rangle$ and $|2\rangle$.

The induced polarization at the probe frequency is $P(\omega_p) = \varepsilon_0\chi(\omega_p)E_p$, where the susceptibility $\chi(\omega_p) = K\rho_{31}/\Omega_p$, $K = N_0|\mu_{31}|^2/\hbar\varepsilon_0$, and N_0 is the atomic density. For a weak probe field ($\Omega_p \ll \Omega_c$, Ω_b, γ_3), we obtain the steady state solution of the off diagonal element ρ_{31} from Eqs. (1e)–(1j)

$$\rho_{31} = -i\Omega_p\frac{A_1 + A_2 + A_3}{M}, \tag{2a}$$

here

$$A_1 = 2(\rho_{33}^{(0)} - \rho_{11}^{(0)})(4\Gamma_{34}\Gamma_{24}\Gamma_{21} + \Gamma_{21}|\Omega_c|^2 + \Gamma_{34}|\Omega_b|^2), \quad (2b)$$

$$A_2 = \frac{1}{2\Gamma_{23}}(\rho_{33}^{(0)} - \rho_{22}^{(0)})(-4\Gamma_{34}\Gamma_{24}|\Omega_c|^2 - |\Omega_c|^4 + |\Omega_c|^2|\Omega_b|^2), \quad (2c)$$

$$A_3 = \frac{1}{2\Gamma_{14}}(\rho_{44}^{(0)} - \rho_{11}^{(0)})(-4\Gamma_{21}\Gamma_{24}|\Omega_b|^2 - |\Omega_b|^4 + |\Omega_c|^2|\Omega_b|^2), \quad (2d)$$

$$M = 16\Gamma_{34}\Gamma_{24}\Gamma_{31}\Gamma_{21} + 4(\Gamma_{34}\Gamma_{24} + \Gamma_{31}\Gamma_{21})|\Omega_c|^2 + 4(\Gamma_{34}\Gamma_{31} + \Gamma_{21}\Gamma_{24})|\Omega_b|^2 + (|\Omega_c|^2 - |\Omega_b|^2)^2, \quad (2e)$$

where $\rho_{11}^{(0)}$, $\rho_{22}^{(0)}$, $\rho_{33}^{(0)}$ and $\rho_{44}^{(0)}$ represent atomic population of corresponding levels (the superscript (0) denotes the zero-order term of the probe field E_p). Closure of the system requires that $\rho_{11}^{(0)} + \rho_{22}^{(0)} + \rho_{33}^{(0)} + \rho_{44}^{(0)} = 1$. If there's no spontaneous decay from $|4\rangle$ to $|2\rangle$ ($\gamma_{42} = 0$ in Eq. (1b)), the steady state population is concentrated in the states $|1\rangle$ and $|4\rangle$ ($\rho_{22}^{(0)} = \rho_{33}^{(0)} = 0$), and ρ_{31} is just determined by A_1 and A_3. We find that $\mathrm{Im}[\rho_{31}]$ is always larger than zero, which represents the absorption of the probe field. When $\gamma_{42} \neq 0$ (the $|2\rangle$–$|4\rangle$ transition is allowed), all the four states have the population distribution and the contribution of A_2 results in the population transfer to the excited state $|3\rangle$, which leads to the amplification of the probe field ($\mathrm{Im}[\rho_{31}] < 0$) under certain conditions. The physical mechanism of the gain has been discussed in Ref. [25].

In order to understand the sub-Doppler spectral features observed in our experiment, we consider the Doppler broadening in the four-level system. For atoms moving with velocity υ, we replace ω_c by $\omega_c - k_c\upsilon$, ω_b by $\omega_b - k_b\upsilon$, and ω_p by $\omega_p - k_p\upsilon$, where k_i is the wave vector of the corresponding laser beam. The susceptibility is averaged over the Maxwell velocity distribution by

$$\chi(\upsilon) = \int [(|\mu_{31}|^2/\hbar\varepsilon_0)\rho_{31}(\upsilon)N(\upsilon)/\Omega_p]\,\mathrm{d}\upsilon, \quad (3a)$$

$$N(\upsilon) = N_0 \mathrm{e}^{-\upsilon^2/u^2}/(u\sqrt{\pi}), \quad (3b)$$

$$u = (2k_B T/M)^{1/2}. \quad (3c)$$

where k_B is the Boltzmann constant, T is the temperature of the gas in the cell, and M is the atomic mass.

Based on Eqs. (1)–(3), we perform numerically calculations of the probe absorption spectra. First, we show the results for $\gamma_{42} = 0$ (the transition between state $|4\rangle$ and state $|2\rangle$ is forbidden). In the actual experimental system, the three hyperfine levels of the excited states $5P_{3/2}$, $F_e = 1$, 2 and 3 are overlapped in the Doppler-broadened absorption profile. In order to make a realistic fit to the experimental results, the numerical plots (dotted lines) in Fig. 4 are calculated by involving six levels (including all the three levels $5P_{3/2}$, $F_e = 1,2,3$ of the excited state $|4\rangle$ as shown in Fig. 1b). We find that the off-resonant coupling of the coupling field E_b with the other two hyperfine levels ($5P_{3/2}$, $F_e = 2$ and 1) results in some asymmetry of the spectra and a small amount of population transfer from the states $|1\rangle$ and $|4\rangle$, but the main spectral features of the four-level system are largely left intact. The underlying physical mechanism can be understood from the four-level system.

We present a simple analysis of the dressed state picture of the four-level system to interpret the spectra presented in Fig. 4. The interaction Hamiltonian for the four-level medium driven by the two coupling fields in the co-propagating configuration is given by [16]

$$H_I = \begin{pmatrix} 0 & 0 & 0 & \frac{-\Omega_b^*}{2} \\ 0 & 0 & \frac{-\Omega_c^*}{2} & 0 \\ 0 & \frac{-\Omega_c}{2} & -k\upsilon & 0 \\ \frac{-\Omega_b}{2} & 0 & 0 & -k\upsilon \end{pmatrix}, \quad (4a)$$

here we assume $k_c \approx k_b \approx k_p = k$ and consider the resonance condition $\Delta_c = \Delta_b = 0$. The eigenvalues for the four dressed states are

$$\lambda_\pm^c = \frac{k\upsilon}{2} \pm \frac{1}{2}\sqrt{(k\upsilon)^2 + |\Omega_c|^2}, \quad (4b)$$

$$\lambda_\pm^b = \frac{k\upsilon}{2} \pm \frac{1}{2}\sqrt{(k\upsilon)^2 + |\Omega_b|^2}. \quad (4c)$$

The probe laser couples the four dressed states and the splittings of the dressed state transitions are given by $\lambda_\pm^c - \lambda_\pm^b$, which are

$$\lambda_1 = -\frac{1}{2}\left(\sqrt{(k\upsilon)^2 + |\Omega_c|^2} + \sqrt{(k\upsilon)^2 + |\Omega_b|^2}\right), \quad (5a)$$

$$\lambda_2 = -\frac{1}{2}\left(\sqrt{(k\upsilon)^2 + |\Omega_c|^2} - \sqrt{(k\upsilon)^2 + |\Omega_b|^2}\right), \quad (5b)$$

$$\lambda_3 = \frac{1}{2}\left(\sqrt{(k\upsilon)^2 + |\Omega_c|^2} - \sqrt{(k\upsilon)^2 + |\Omega_b|^2}\right), \quad (5c)$$

$$\lambda_4 = \frac{1}{2}\left(\sqrt{(k\upsilon)^2 + |\Omega_c|^2} + \sqrt{(k\upsilon)^2 + |\Omega_b|^2}\right). \quad (5d)$$

The dressed state transitions correspond to the four absorption peaks. Eqs. (5b) and (5c) show that λ_2 and λ_3 correspond to the two center peaks and are not shifted much with $k\upsilon$ due to the partial cancellation of the Doppler shift term $k\upsilon$, which leads to the two sub-Doppler absorption peaks as shown in Fig. 4a, b and d (two narrowing absorption peaks in the middle). In contrast, λ_1 and λ_4 are shifted dramatically with changing $k\upsilon$ as shown by Eqs. (5a) and (5d) and the two dressed state transitions are fully Doppler-broadened as shown in Fig. 4(a)–(d) (two broadening absorption peaks on both sides). In Fig. 4a, b and d, there is a narrow dip between two narrow peaks in the center. The depth and the width of the dip depend on the relative value of the two Rabi frequencies Ω_b and Ω_c. The separation of the two peaks is proportional to $|\lambda_3 - \lambda_2| = |\sqrt{(k\upsilon)^2 + \Omega_c^2} - \sqrt{(k\upsilon)^2 + \Omega_b^2}|$. In our experiment, we find that as the intensities of the two coupling lasers become nearly equalized, the two narrow peaks are not resolved and just one narrow peak appears in the center. When $\Omega_b = \Omega_c$, $\lambda_2 = \lambda_3 = 0$, the two dressed states

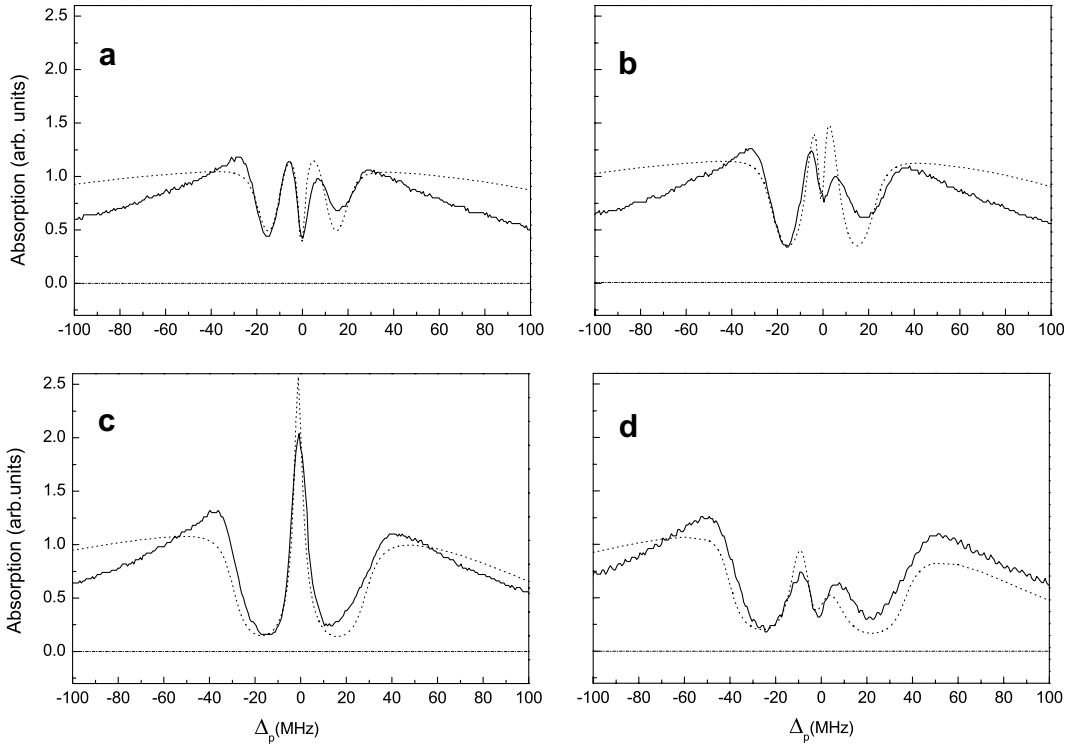

Fig. 4. The solid lines are measured probe absorption spectra versus the probe frequency detuning Δ_p. The coupling laser E_c is tuned on resonance with the $5S_{1/2}$, $F_g = 1 \rightarrow 5P_{1/2}$, $F_e = 2$ transition and has an intensity of 34 mW/cm^2. The coupling laser E_b is tuned to the resonance of the $5S_{1/2}$, $F_g = 2 \rightarrow 5P_{3/2}$, $F_e = 3$ transition with an intensity of: (a) ~3 mW/cm^2, (b) ~12 mW/cm^2, (c) ~34 mW/cm^2 and (d) ~90 mW/cm^2. The dotted lines are the theoretical calculations based on the four-level system including all the three hyperfine levels of the excited states $5P_{3/2}$, $F_e = 1$, 2 and 3. The fitting parameters are $\gamma_3/2\pi = \gamma_4/2\pi = \gamma/2\pi = 10$ MHz, $\gamma_{21} = 0.1\gamma$, $\Omega_c = 1.5\gamma$, $\Omega_b = 0.45\gamma$, 0.8γ, 1.5γ and 2.5γ in (a), (b), (c) and (d), respectively.

in the middle become degenerate, a narrower and higher absorption peak appears in the center as shown in Fig. 3b (Fig. 4c). The spectral peak at $\lambda_2 = \lambda_3 = 0$ is therefore free from the Doppler shift. We note that the simple dressed state picture explains Doppler shift and does not provide the spectral linewidths. In fact, theoretical calculations [21,23] show that the Doppler effect actually narrows the spectral peaks to below the natural linewidth when contributions from different pump and probe detunings are all included. The measured linewidth of the narrow central peak in Fig. 3b (Fig. 4c) is about 10 MHz, which is larger than the natural linewidth of 5.3 MHz for the ^{87}Rb excited state level $|3\rangle$ ($5P_{1/2}$) and can be attributed to the broadening effects of the finite laser linewidth, the transit time of the atoms across the laser beams (γ_{21}), the spatial inhomogeneity of the coupling laser intensities, and the Zeeman broadening from the residual magnetic field. The unit γ in the theoretical plots is chosen $2\pi \times 10$ MHz and results in the best fit to the experimental data.

The calculations for $\gamma_{42} \neq 0$ (the transition $|4\rangle \rightarrow |2\rangle$ is allowed) including all the three levels ($5P_{3/2}$, $F_e = 1, 2, 3$) of the excited state $|4\rangle$ are plotted in Fig. 5 as dotted lines while the experimental results are plotted in solid lines. The underlying physical mechanism of this case can be understood by considering the coupling field E_b as a perturbing field for the three-level ($|1\rangle$–$|2\rangle$–$|3\rangle$) EIT system as discussed in Ref. [25]. From numerical calculations we find that the atoms with different velocities all contribute more or less to the dip at the central resonance and the weighted average from Eq. (3a) forms the narrow dip. Comparing the experimental results with the numerical calculations in Fig. 5, we can see that the measured linewidth of the absorption dip is narrower than that of the numerical calculations. Especially for Fig. 5b, the measured linewidth is nearly unaffected by increasing the intensity of coupling field E_b. This can be explained by the nonlinear behavior due to the Doppler broadening and the optical pumping as discussed in Ref. [26]. We note that when the transition $|4\rangle \rightarrow |2\rangle$ is allowed, the four-wave mixing (FWM) process in the four-level system becomes possible as discussed in Refs. [9,10]. In our experimental system, due to the limited optical density length and the weak probe field, the nonlinear FWM signal at $|4\rangle \rightarrow |2\rangle$ transition is therefore very weak and the FWM contribution to the probe field should not be dominant.

It is interesting to note that at larger Rabi frequencies Ω_b and Ω_c, a double dip structure may appear in the calculated probe spectrum as shown in Fig. 6. This is similar to the double peak structure predicted at the high pump intensity for the N type system (no decay from the state $|4\rangle$ to the state $|2\rangle$) [21]. In Fig. 6, the solid lines of the insets are the expanded view of the central absorption dip calculated by including all the three hyperfine levels ($5P_{3/2}$, $F_e = 1, 2, 3$) of the excited state $|4\rangle$, and the dotted lines are the calcula-

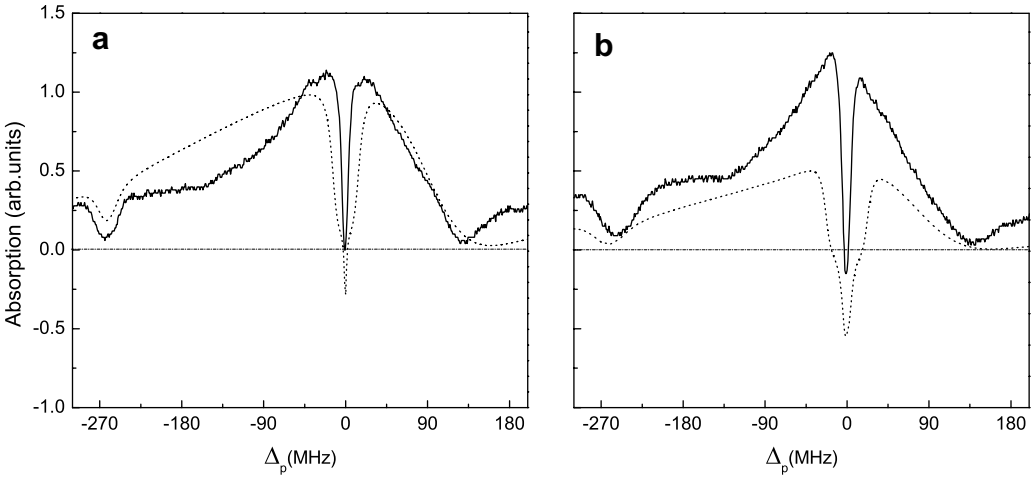

Fig. 5. The solid lines are measured probe absorption spectra versus the probe frequency detuning Δ_p. The coupling laser E_c is tuned on resonance with the $5S_{1/2}$, $F_g = 1 \rightarrow 5P_{1/2}$, $F_e = 2$ transition and has an intensity of 18 mW/cm^2. The coupling laser E_b is tuned to the resonance of the $5S_{1/2}$, $F_g = 2 \rightarrow 5P_{3/2}$, $F_e = 2$ transition with an intensity of: (a) ~18 mW/cm^2 and (b) ~32 mW/cm^2. The dotted lines are the theoretical calculations based on the four-level system including all the three hyperfine levels of the excited states $5P_{3/2}$, $F_e = 1$, 2 and 3. The fitting parameters are $\gamma_3/2\pi = \gamma_4/2\pi = \gamma/2\pi = 10$ MHz, $\gamma_{21} = 0.1\gamma$, $\Omega_c = 0.8\gamma$, $\Omega_b = 0.8\gamma$ and 1.4γ in (a) and (b), respectively.

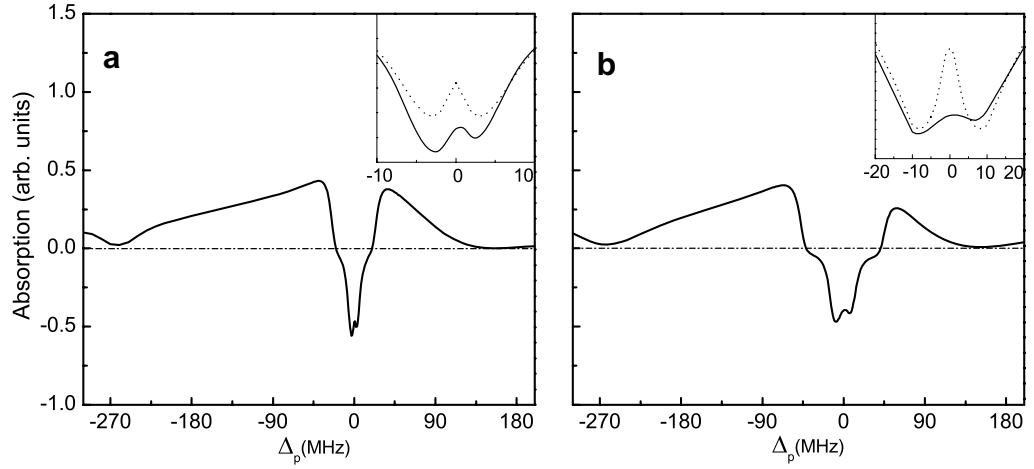

Fig. 6. Calculated probe absorption spectra versus the probe frequency detuning Δ_p for the same case as Fig. 5. The solid lines of the insets are the expanded view of the central absorption dip calculated by including all the three hyperfine levels ($5P_{3/2}$, $F_e = 1, 2, 3$) of excited state $|4\rangle$. The dotted lines are the plots for the basic four-level system. The parameters are $\gamma_3/2\pi = \gamma_4/2\pi = \gamma/2\pi = 10$ MHz, $\gamma_{21} = 0.1\gamma$, and $\Omega_c = 0.8\gamma$, $\Omega_b = 1.6\ \gamma$ in (a), $\Omega_c = 1.5\gamma$, $\Omega_b = 3\gamma$ in (b).

tions for the basic four-level system. We can see that the off-resonant coupling of the coupling field E_b with the other two hyperfine levels ($5P_{3/2}$, $F_e = 1$ and 3) lowers the small peak of the absorption dip, but does not destroy the structure. However, the double dip spectrum is not observed in our experiment. We believe that the effects from the magnetic sublevels of ^{87}Rb hyperfine states such as the population redistribution in different magnetic sublevels and the Zeeman broadening prevent us from observing the detailed double dip structure under our experimental conditions.

These two different spectral features under the two conditions (without and with spontaneous decay from $|4\rangle$ to $|2\rangle$) are also observed when the two coupling lasers are detuned from their respective resonances. When the second coupling field E_b is tuned on resonance with the $5S_{1/2}$, $F_g = 2 \rightarrow 5P_{3/2}$, $F_e = 2$ transition and the first coupling field E_c is turned off, the ^{87}Rb system becomes a three-level V type system. But it is not a simple three-level V system because of the three hyperfine levels ($5P_{3/2}$, $F_e = 1, 2, 3$) of the excited state $|4\rangle$. In Fig. 7a, the central dip (at $\Delta_p = 0$) corresponds to the resonant three-level V system (the $5P_{3/2}$, $F_e = 2 \rightarrow 5S_{1/2}$, $F_g = 2 \rightarrow 5P_{1/2}$, $F_e = 2$ transitions). The left dip of Fig. 7a (at $\Delta_p \sim -267$ MHz) corresponds the off-resonant coupled V system (the $5P_{3/2}$, $F_e = 3 \rightarrow 5S_{1/2}$, $F_g = 2 \rightarrow 5P_{1/2}$, $F_e = 2$ transitions). The right dip of Fig. 7a (at $\Delta_p \sim 157$ MHz) corresponds to another off-resonant coupled V system (the $5P_{3/2}$, $F_e = 1 \rightarrow 5S_{1/2}$, $F_g = 2 \rightarrow 5P_{1/2}$, $F_e = 2$ transitions). The two relatively broad dips in Figs. 3c and 5 are there for the same reason discussed here. If we detune the first coupling field E_c from the $5S_{1/2}$, $F_g = 1 \rightarrow 5P_{1/2}$, $F_e = 2$ transition with $\Delta_c \approx -267$ MHz and $\Delta_c \approx 157$ MHz, respectively, we

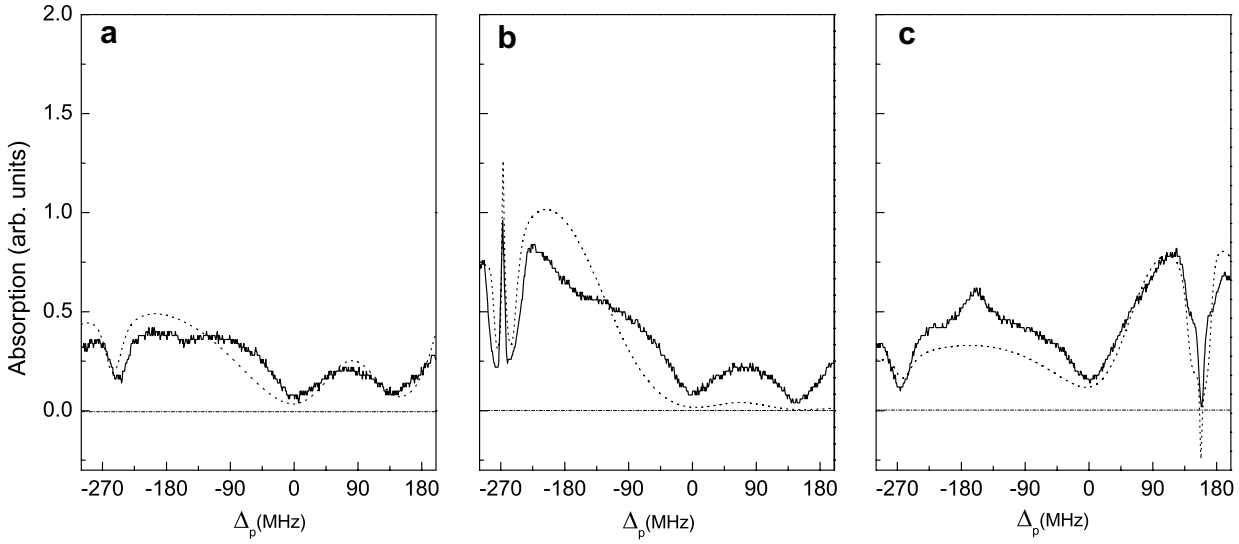

Fig. 7. The solid lines are measured probe absorption spectra versus the probe frequency detuning Δ_p. The second coupling laser E_b is always kept on resonance with the $5S_{1/2}$, $F_g = 2 \rightarrow 5P_{3/2}$, $F_e = 2$ transition and its intensity is 18 mW/cm^2: (a) the first coupling field E_c is turned off and the probe spectrum corresponds to that of a three-level V type system. The first coupling laser E_c (with an intensity 18 mW/cm^2) is detuned from the $5S_{1/2}$, $F_g = 1 \rightarrow 5P_{1/2}$, $F_e = 2$ transition by $\Delta_c = -267$ MHz in (b), and by $\Delta_c = 157$ MHz in (c). The dotted lines are the theoretical calculations based on the four-level system including all the three hyperfine levels of the excited states $5P_{3/2}$, $F_e = 1$, 2 and 3. The fitting parameters are $\gamma_3/2\pi = \gamma_4/2\pi = \gamma/2\pi = 10$ MHz, $\gamma_{21} = 0.1\gamma$, $\Delta_b = 0$, $\Omega_b = 0.8\gamma$, and $\Omega_c = 0.8\gamma$.

observe the narrow absorption peak (at $\Delta_p \approx -267$ MHz) and dip (at $\Delta_p \approx 157$ MHz) shown in Fig. 7b and c, respectively, which are similar to the absorption peak and dip observed at $\Delta_p = 0$ in Fig. 3b and c for the resonantly coupled four-level system. The dotted lines in Fig. 7 are the calculated probe absorption for (a) $\Omega_c = 0$, (b) $\Delta_c = -267$ MHz, and (c) $\Delta_c = 157$ MHz, respectively, which agree well with the experimental results. It is shown in Ref. [23] that when the coupling lasers are detuned, the two-photon Raman resonance dominates, and the Doppler narrowing effect is more striking. With the Doppler effect, the population distribution among the four levels depends on the detuning and the atomic velocity. When $\Delta_c = \Delta_p = -267$ MHz (157 MHz), the two-photon coupling $5P_{3/2}$, $F_e = 3$ (1) $\rightarrow 5S_{1/2}$, $F_g = 2 \rightarrow 5P_{1/2}$, $F_e = 2$ in the V system and the two-photon coupling $5S_{1/2}$, $F_g = 2 \rightarrow 5P_{1/2}$, $F_e = 2 \rightarrow 5S_{1/2}$, $F_g = 1$ in the Λ system are simultaneously resonant for all atoms, which leads to the sub-Doppler absorption peak at $\Delta_p = -267$ MHz (the sub-Doppler amplification dip at $\Delta_p = 157$ MHz). For other values of the detuning Δ_c, the resonance conditions can not be met simultaneously for the V and Λ systems, the sub-Doppler absorption peak (the sub-Doppler amplification dip) at $\Delta_p = \Delta_c$ disappears, only the EIT dip produced in the coupled Λ system exists at $\Delta_p = \Delta_c$, and this is demonstrated by the numerical calculation and also observed in our experiment.

3. Conclusion

We have explored the sub-Doppler spectral resolution in a Doppler-broadened ^{87}Rb atomic sample coherently coupled by two intense laser fields and probed by a weak laser field. The laser-coupled ^{87}Rb system can be viewed as a quasi four-level N type system and the probe absorption spectrum exhibits interesting sub-Doppler features. When there is no spontaneous population transfer among the two sets of the transitions connected by the two intense laser fields, the observed probe spectrum exhibits two sub-Doppler peaks and a narrow dip near the probe resonance. In particular, the two sub-Doppler peaks collapse into a single narrow peak at the center of the Doppler-broadened absorption profile when the Rabi frequencies of the two intense lasers are equal to each other. On the other hand, when there is the spontaneous population transfer among the two sets of the transitions connected by the two intense laser fields, the probe absorption spectrum exhibits a narrow sub-Doppler dip in the center of the Doppler-broadened absorption profile and the sub-Doppler amplification of the probe laser can be observed by controlling the intensities of the two intense lasers. Because the three hyperfine levels of the ^{87}Rb $5P_{3/2}$ state are smaller than the Doppler width, the sub-Doppler spectra can be observed by varying the detuning of the laser frequencies to match the hyperfine splittings. The analytical and numerical calculations based on the four-level N type model have been presented to explain the experimental results and agree well with the experimental measurements. The sub-Doppler spectral resolution may be useful in high-resolution spectroscopy and in gas-cell atomic frequency standards. Also the steep variation of the light dispersion associated with the narrow absorptive peaks and dips may be used for controlling the light group velocities.

Acknowledgements

This work is supported by the National Natural Science Foundation of China under Grant No. 10474119, by the National Basic Research Program of China under Grant No. 001CB309309, and also by funds from the Chinese Academy of Sciences. Y.Z. acknowledges support from the National Science Foundation.

References

[1] S.E. Harris, Phys. Today 50 (7) (1997) 36.
[2] M. Fleischhauer, A. Imamoglu, J.P. Marangos, Rev. Mod. Phys. 77 (2005) 633.
[3] E. Arimondo, G. Orriols, Nuovo Cimento Lett. 17 (1976) 333;
H.R. Gray, R.M. Whitley, C.R. Stroud, Opt. Lett. 3 (1989) 218;
E. Arimondo, in: E. Wolf (Ed.), Progress in Optics, vol. XXXV, Elsevier Science, Amsterdam, 1996, p. 259.
[4] M.O. Scully, S.Y. Zhu, A. Gavrielides, Phys. Rev. Lett. 62 (1989) 2813;
S.E. Harris, Phys. Rev. Lett. 62 (1989) 1033;
O.A. Kocharovskaya, Phys. Rep. 219 (1992) 175;
M.O. Scully, Phys. Rep. 219 (1992) 191;
Jinyue Gao et al., Opt. Commun. 93 (1992) 323;
A.S. Zibrov, M.D. Lukin, D.E. Nikonov, L. Hollberg, M.O. Scully, V.L. Velichansky, H.G. Robinson, Phys. Rev. Lett. 75 (1995) 1499.
[5] L.V. Hau, S.E. Harris, Z. Dutton, C.H. Behroozi, Nature (London) 397 (1999) 594;
M.M. Kash, V.A. Sautenkov, A.S. Zibrov, L. Hollberg, G.R. Welch, M.D. Lukin, Y. Rostovtsev, E.S. Fry, M.O. Scully, Phys. Rev. Lett. 82 (1999) 5229;
D. Budker, D.F. Kimball, S.M. Rochester, V.V. Yashchuk, Phys. Rev. Lett. 83 (1999) 1767.
[6] L.J. Wang, A. Kuzmich, A. Dogariu, Nature (London) 407 (2000) 277;
A.M. Akulshin, S. Barreiro, A. Lezama, Phys. Rev. Lett. 83 (1999) 4277;
K. Kim, H.S. Moon, C. Lee, S.K. Kim, J.B. Kim, Phys. Rev. A 68 (2003) 013810.
[7] D.F. Phillips, A. Fleischhauer, A. Mair, R.L. Walsworth, M.D. Lukin, Phys. Rev. Lett. 86 (2001) 783;
C. Liu, Z. Dutton, C.H. Behroozi, L.V. Hau, Nature (London) 409 (2001) 490;
J.J. Longdell, E. Fraval, M.J. Sellars, N.B. Manson, Phys. Rev. Lett. 95 (2005) 063601.
[8] S.E. Harris, J.E. Field, A. Imamoglu, Phys. Rev. Lett. 64 (1990) 1107;
H. Schmidt, A. Imamoglu, Opt. Lett. 21 (1996) 1936;
S.E. Harris, Y. Yamamoto, Phys. Rev. Lett. 81 (1998) 3611;
S.E. Harris, L.V. Hau, Phys. Rev. Lett. 82 (1999) 4611;
M.D. Lukin, S.F. Yelin, M. Fleischhauer, Phys. Rev. Lett. 84 (2000) 4232;
H. Kang, Y. Zhu, Phys. Rev. Lett. 91 (2003) 093601;
A. Andre, M. Bajcsy, A.S. Zibrov, M.D. Lukin, Phys. Rev. Lett. 94 (2005) 063902;
Danielle A. Braje, Vlatko Balic, G.Y. Yin, S.E. Harris, Phys. Rev. A 68 (2003) 041801(R).
[9] S.A. Babin, E.V. Podivilov, D.A. Shapiro, U. Hinze, E. Tiemann, B. Wellegehausen, Phys. Rev. A 59 (1999) 1355;
U. Hinze, L. Meyer, B.N. Chichkov, E. Tiemann, B. Wellegehausen, Opt. Commun. 166 (1999) 127;
M.T. Johnsson, E. Korsunsky, M. Fleischhauer, Opt. Commun. 212 (2002) 335.
[10] Danielle A. Braje, Vlatko Balic, Sunil Goda, G.Y. Yin, S.E. Harris, Phys. Rev. Lett. 93 (2004) 183601.
[11] G. Vemuri, G.S. Agarwal, B.D. Nageswara Rao, Phys. Rev. A 53 (1996) 2842;
Y. Zhu, T.N. Wasserlauf, Phys. Rev. A 54 (1996) 3653.
[12] G.S. Agarwal, W. Harshawardhan, Phys. Rev. Lett. 77 (1996) 1039.
[13] Y. Zhu, J. Lin, Phys. Rev. A 53 (1996) 1767;
G. Vemuri, G.S. Agarwal, B.D. Nageswara Rao, Phys. Rev. A 54 (1996) 3695.
[14] A.K. Popov, V.M. Shalaev, Phys. Rev. A 59 (1999) R946;
A.K. Popov, A.S. Bayev, Phys. Rev. A 62 (2000) 025801.
[15] Po Dong, A.K. Popov, Sing Hai Tang, Jin-Yue Gao, Opt. Commun. 188 (2001) 99.
[16] C.Y. Ye, A.S. Zibrov, Y.V. Rostovtsev, M.O. Scully, Phys. Rev. A 65 (2002) 043805.
[17] S.F. Yelin, V.A. Sautenkov, M.M. Kash, G.R. Welch, M.D. Lukin, Phys. Rev. A 68 (2003) 063801;
C. Goren, A.D. Wilson-Gordon, M. Rosenbluh, H. Friedmann, Phys. Rev. A 69 (2004) 063802.
[18] A.M. Akulshin, S. Barreiro, A. Lezama, Phys. Rev. A 57 (1998) 2996;
A. Lezama, S. Barreiro, A.M. Akulshin, Phys. Rev. A 59 (1999) 4732.
[19] A.V. Taichenachev, A.M. Tumaikin, V.I. Yudin, Phys. Rev. A 61 (1999) 011802(R).
[20] C. Goren, A.D. Wilson-Gordon, M. Rosenbluh, H. Friedmann, Phys. Rev. A 67 (2003) 033807.
[21] C. Goren, A.D. Wilson-Gordon, M. Rosenbluh, H. Friedmann, Phys. Rev. A 69 (2004) 053818.
[22] C. Goren, A.D. Wilson-Gordon, M. Rosenbluh, H. Friedmann, Phys. Rev. A 70 (2004) 043814.
[23] A.S. Zibrov, A.B. Matsko, JETP Lett. 82 (2005) 472.
[24] E.A. Wilson, N.B. Manson, C. Wei, Phys. Rev. A 67 (2003) 023812.
[25] Hoonsoo Kang, Lingling Wen, Yifu Zhu, Phys. Rev. A 68 (2003) 063806.
[26] C.Y. Ye, A.S. Zibrov, Phys. Rev. A 65 (2002) 023806.